ISSN 2581 – 3781

AJCSE
ASIAN JOURNAL OF COMPUTER SCIENCE ENGINEERING

Available Online at www.ajcse.info
Asian Journal of Computer Science Engineering 2021;6(3):8-17

RESEARCH ARTICLE

Contactless Real-Time Vital Signs Monitoring Using a Webcam

Duaa H. Ali, Mazin H. Aziz

Department of Computer Engineering, University of Mosul, Mosul, Iraq

Received on: 15-06-2021; Revised on: 20-07-2021; Accepted on: 19-08-2021

ABSTRACT

Measurement of vital signs such as heart rate (HR), respiratory rate (RR), blood pressure (BP), and oxygen saturation (SpO_2) is important for everyone in recent years due to the spread of epidemic diseases such as SARS and Coronavirus disease-19. This study presents methods to measure the four vital signs (HR, RR, BP, and SpO_2) simultaneously, contactless, and in real-time from facial video using a webcam. The estimation of the four vital signs in our study is based on photoplethysmography (PPG) extracted from the skin. There are many studies that dealt with the measurement of vital signs from PPG, but our study was distinguished from them by estimating and monitoring the four vital signs together in real-time and in less initial time takes 6 s only with good results where the maximum error is: ±4, ±2.2, ±3, ±1, and ±2 for HR, RR, systolic BP (SP), diastolic BP (DP), and SpO_2, respectively.

Key words: Heart rate, Respiratory rate, Blood pressure, Oxygen saturation, Coronavirus disease-19, Facial video

INTRODUCTION

In biomedical metrology, the measurement of vital signs such as heart rate (HR), respiratory rate (RR), blood pressure (BP), and oxygen saturation (SpO2) is a basic task in the diagnosis and management of diseases.[1-3] Conventional devices for these tasks are based on contact approaches mostly, which have several drawbacks. Foremost, contact with the body and skin raises the risk of skin irritation and germ contamination. Moreover, these devices limit the patient's body movement, accordingly, can lead to severe inconveniences. Therefore, the contactless estimation of vital signs using a camera is constantly gaining importance due to its advantages in terms of hygiene and patient convenience.

In 1995, Costa *et al*. studied the first contactless safety monitoring system.[4] They used camera images to derive physiological parameters with the help of skin color variability. However, their approaches did not report quantitative results; they only reported a graph of heartbeats. Following this first attempt, development was moderate and in 2005 another innovative approach was implemented using a thermal camera for measuring the emotional state of the computer user using the facial thermal image.[5] Takano *et al*. showed in 2006 that more than a single physiological parameter can be estimated simultaneously using a camera but their system's efficiency was unknown.[6] In recent years, researchers that using photoimaging images to estimate vital signs using advanced image and signal processing techniques have increased dramatically.[7-16]

To develop viable systems for video-based health sign monitoring, the application environment must be defined first, followed by the necessary system parameters and processing algorithms, as well as display methods.[17]

In this study, we propose a real-time health care monitoring system via a webcam for indoor and outdoor personal use. Given the Coronavirus disease-19 outbreak, it can be also used to ensure the safety of employees when they come to work. Our proposed methods can monitor HR, RR, BP, and SpO_2 together for one individual only at the same time.

HR

The heart is the most essential muscle organ in the human body, controlling blood flow throughout

Address for correspondence:
Duaa H. Ali,
E-mail: duaa.hussein.ali94@gmail.com

the entire body. The HR points to the number of times a heart pulses in 1 min.[18] The HR evaluates a heart's strength and performance. Different sensory equipment such as a Doppler probe,[19] a pulse oximeter,[20] and an electrocardiogram (ECG) machine[21] used to monitor HR. The normal range of HR at resting is 60–80 beats per minute (bpm) for healthy adults,[22] while in children vary depending on their age.[23] Many various attempts have been reported in the literature to contactless HR measurement using a webcam,[24-30] a thermal camera,[31] a charge coupled device camera,[32] a Complementary Metal Oxide Semiconductor camera,[33] and a smartphone camera.[34] Driver monitoring, sleep monitoring, newborn and elderly monitoring, emotional and stress detection, telemedicine, etc., are some of the clinical and non-clinical applications of contactless HR monitoring through a camera.[17]

RR

RR is the number of breaths per minute.[35] The normal range of RR at rest is 12–20 breaths per minute for healthy adults,[36,37] whereas normal values for children change depending on their age.[23] The RR can be measured by counting the number of breaths take during the course of 1 min at rest.[38] This method needs time, attention and is impractical in continuous monitoring. Electrophysiological tests[39] similar to ECG and pressure sensors[40,41] are commonly used in contact-based RR measurements. Ultrasound[42-47] or microwave[48] measurements are commonly used in non-contact testing procedures. In recent years, interest has emerged in monitoring RR using a camera,[49-60] whereas the studies are still few and need further improvement.

BP

BP is the force that blood exerts on the walls of blood vessels expressed in millimeters of mercury (mmHg). It consists of two parts: Systolic BP (SBP) and diastolic BP (DP). SBP is the pressure of the blood on the vessels' walls during heart beats, while DP is the pressure of the blood on the vessels' walls during heart rest. The normal range of SBP is (90–120 mmHg) and of DP is (60–80 mm Hg).[61] A Conventional device to measure BP is a sphygmomanometer that has three major types: Mercury, digital, and aneroid.[62] Recently, the number of studies that attended on BP measurement via video images has increased,[63-68] because cuff-based measurement systems capture only a current BP value, which can be easily influenced by stress, nutrition, medicines, age, exercise, and other factors.

Blood SpO_2

Blood SpO_2 is the ratio between oxygen-carrying hemoglobin (Hb) (oxyhemoglobin [HbO_2]) and the total Hb amount in the blood:[69]

$$SpO_2 = \frac{HbO_2}{HbO_2 + Hb} \quad (1)$$

Where HbO_2 and Hb are HbO_2 and deoxyhemoglobin, respectively. The normal range of SpO_2 is 94–100% for healthy persons.[70] Conventional devices to measure the SpO_2 are the pulse oximeter[71-73] and the gas chromatograph,[74] which is the gold standard. The gas chromatograph analyzes arterial blood extracted by a specialist,[74] while the pulse oximeter performs noninvasive measurement based on the absorption properties of HbO_2 and Hb to absorb light at different wavelengths.[73] It is equipped with two infrared (940 nm) and red (600 nm) wavelength light-emitting diode (LEDs), a light detector, and a microprocessor. HbO_2 absorbs infrared light and Hb absorbs red light.[73]

The absorption coefficients determine the ability of one mole of the HbO_2 and the Hb to absorb light at a specific wavelength.[75] Figure 1 shows the absorption coefficients of the $HbO_2$and the Hb versus different light wavelengths.[76]

In Scully *et al*.[14] a smartphone camera is used as a detector and an LED as a light source. By decomposing each frame in the red and blue color channels, the HbO_2 and Hb are extracted. In Scharf, Verkruysse *et al*.[75,77] it was evaluated that wavelengths in the green channel are absorbed by the HbO_2 more than those in the blue.

The wavelength range of the RGB channels of the camera is (370, 950) nm. At the wavelength 600 nm and940 nm, the HbO_2 and the Hb show the greater difference in absorption.[78] These wavelengths match that used in the pulse oximeter. Therefore, in this study, we are proposed to extract the green PPG at the wavelength 600 nm and the red PPG at 940 nm to evaluate the SpO_2 by monitoring the

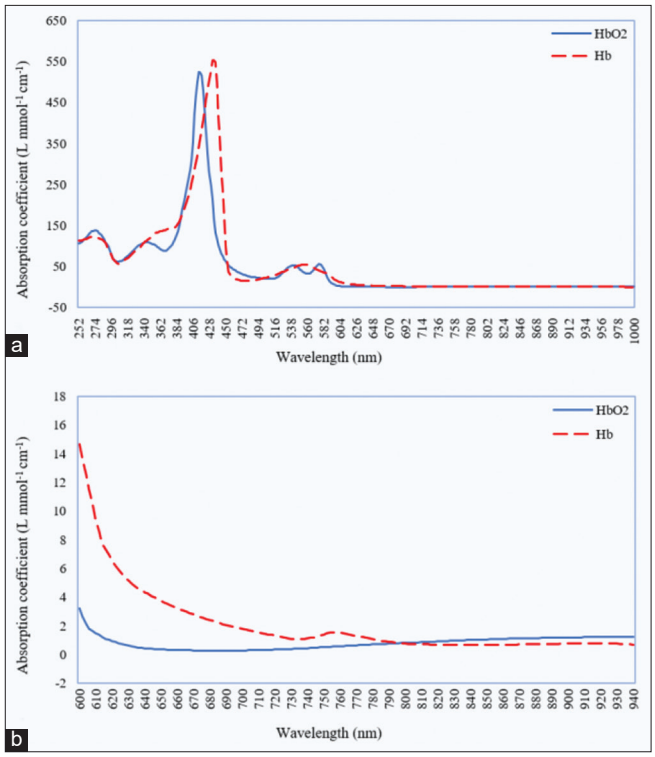

Figure 1: The absorption coefficients of the HbO_2 and the Hbversusdifferent light wavelengths: (a) From 252 nm to1000 nm. (b) Zoom in (a) from 600 nm to 940 nm

variance of the light intensity in the green and red channels of the facial video frames.

Experiments

Dataset

We searched for a public dataset that provides ground-truth values for all four vital signs: HR, RR, SpO_2, and BP together, but we did not find, therefore we made our local dataset to evaluate the performance of our methods. All videos were recorded in 24-bit RGB color space, 30 frames per second (fps), 640 × 480 pixel resolution, 20 s length and saved in mp4 format.

The dataset consists of 42 facial-video for ten healthy volunteers (three males and seven females) between the ages of 13 and 60 years. Each volunteer had at least three videos in this dataset, each of which was recorded with different illumination, one outdoors with indirect ambient sunlight and two indoors with and without fluorescent ambient light. The HR and SpO_2 for each volunteer were measured by a fingertip pulse oximeter during the video recording; the BP was measured before and after recording using a conventional sphygmomanometer, while the RR was computed by the volunteers during the recording.

Experimental Setup

We used a USB stream webcam (Vitade 960A) with built-in ring light adjustable in three brightness for video capturing. It has the following specifications: 80° wide-angle lens captures, automatic correction for illumination, H.264 encoding compression, pixel resolution of 1920 × 1080 pixels, and 30 fps. MSI laptop (core i7, 16 GB RAM) was used in processing proposed methods and display the results.

For ground-truth HR, SpO_2, and BP measurement, a fingertip pulse oximeter was used for HR and SpO_2, which its accuracy is: SpO_2 (70~100%: ±2%; ≤70%: unspecified), HR (±3 bpm), while a mercury sphygmomanometer was used for BP that produce the most accurate results than other sphygmomanometers.

We connected the webcam to the laptop and configured the webcam settings in preparation for the video recording, then asked the volunteers to sit on a chair opposite the webcam approximately 0.5 meters (m) away and put a pulse oximeter on their left index finger and asked a technical person to measure the BP of the volunteers by the sphygmomanometer. We turned on the pulse oximeter and started recording the video at the same time we asked the volunteers to start to compute their RR, we also asked them to commit to as little movement as possible in the first 6 s and then they can do small movements like slight head movements, after 20 s we stopped the recording and saved the video on the laptop.

At least three videos were recorded for each volunteer, each video under different illumination conditions: indoors with fluorescent ambient light and the second brightness of the webcam, indoors with natural ambient light and the second brightness of the webcam, and outdoors with indirect ambient sunlight.

For videos recording, python script with open computer vision (OpenCV) library is used.

METHODS

All the vital signs were found from the extracted photoplethysmography (PPG) signals. At the first, we apply Discriminative Response Map Fitting[79] method on each frame to find the coordinates of 68-facial landmarks for an individual's face detection and tracking. From the detected 68-facial landmarks, we determined the location of the cheeks

with two rectangles that change in size according to the pose of the face as shown in Figure 2. The two rectangles represent the regions of interest (ROI) whose contains pixels of facial-skin that color values change with HR, RR, and the ratio of oxygen in the blood. From the ROI, we extracted the RGB PPG signals shown in Figure 3 by averaging the RGB channels that were decomposed from each frame.

HR and RR

The green channel contains the strongest PPG signal among RGB channels;[77,80] therefore, we used it in both HR and RR estimation.

At the first, detrending was applied on the green PPG signal to alleviate the non-stationary trend caused by motion and illumination as shown in Figure 4. After that, the time-series data were converted to its frequency spectrum by applying Fast Fourier Transform then take the absolute of it as shown in Figure 5a and b, respectively. The frequency spectrum was filtered by a bandpass filter with cutoff frequencies: 0.8–2 Hz and 0.16–0.5 Hz corresponding to the interesting ranges for the HR and RR, respectively. The frequency of the highest peak in each filtered spectrum represents the frequency of the HR and RR as shown in Figure 5c and d, respectively. HR and RR are calculated as shown in equation (2) and equation (3), respectively:

$$HR\ (bpm) = f_{HR} \times 60 \quad (2)$$

$$RR = f_{RR} \times 60 \quad (3)$$

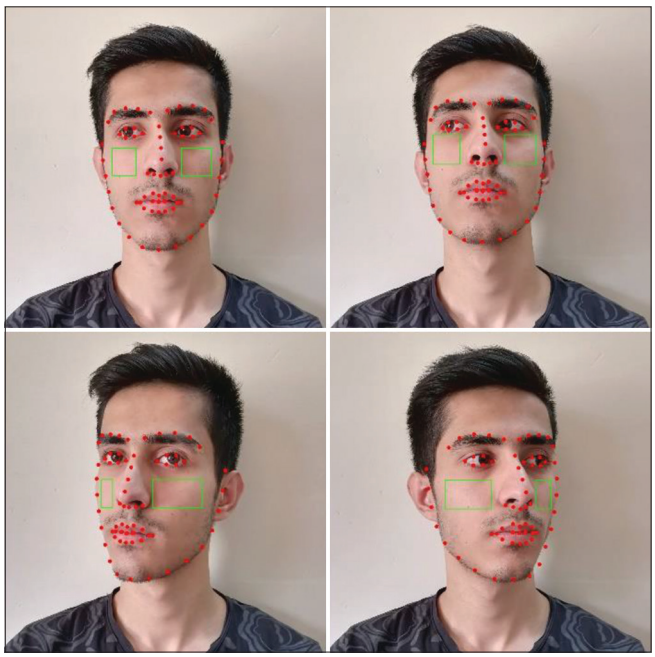

Figure 2: Face and regions of interest (ROI) detection and tracking. The red points indicate the 68 landmarks and the light-green rectangles represent the ROI

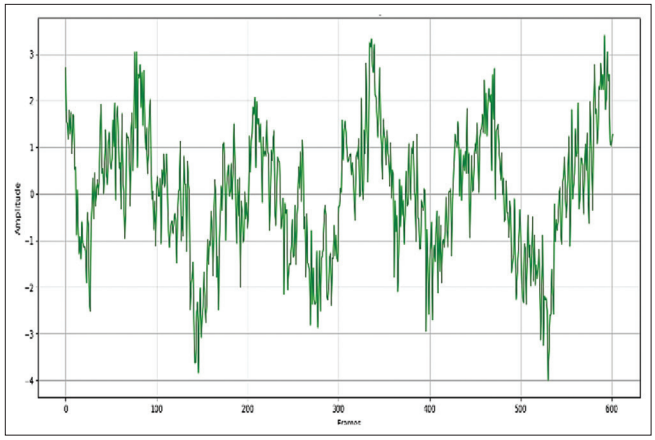

Figure 3: Photoplethysmography signals for the blue, green, and red channels

BP

Bp is affected by several factors, the most important of which are peripheral resistance (R) and cardiac output (CO). Age, gender, weight, and height are other factors affecting BP. R is the resistance of the vessels to blood flow that creates BP. CO is the amount of blood the heart pumps through the circulatory system in 1 min which is usually measured in units of Liter/minute (L/min) and calculated using HR times stroke volume (SV) as shown in equation (4).[81] The average healthy male CO value in the resting is 5 L/min, while in female is 4.5 L/min.[81]

$$CO\ (L/min) = HR \times SV \quad (4)$$

SV is the volume of pumped blood from the heart in one beat. It is found using equation (4) as:

$$SV\,(mL) = \frac{CO}{HR} \times 1000 \quad (5)$$

Pulse pressure (PP) is the difference between SBP and DP:

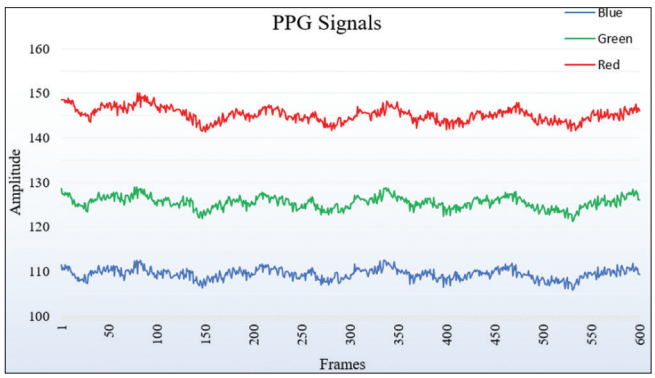

Figure 4: Green photoplethysmography signal after detrending

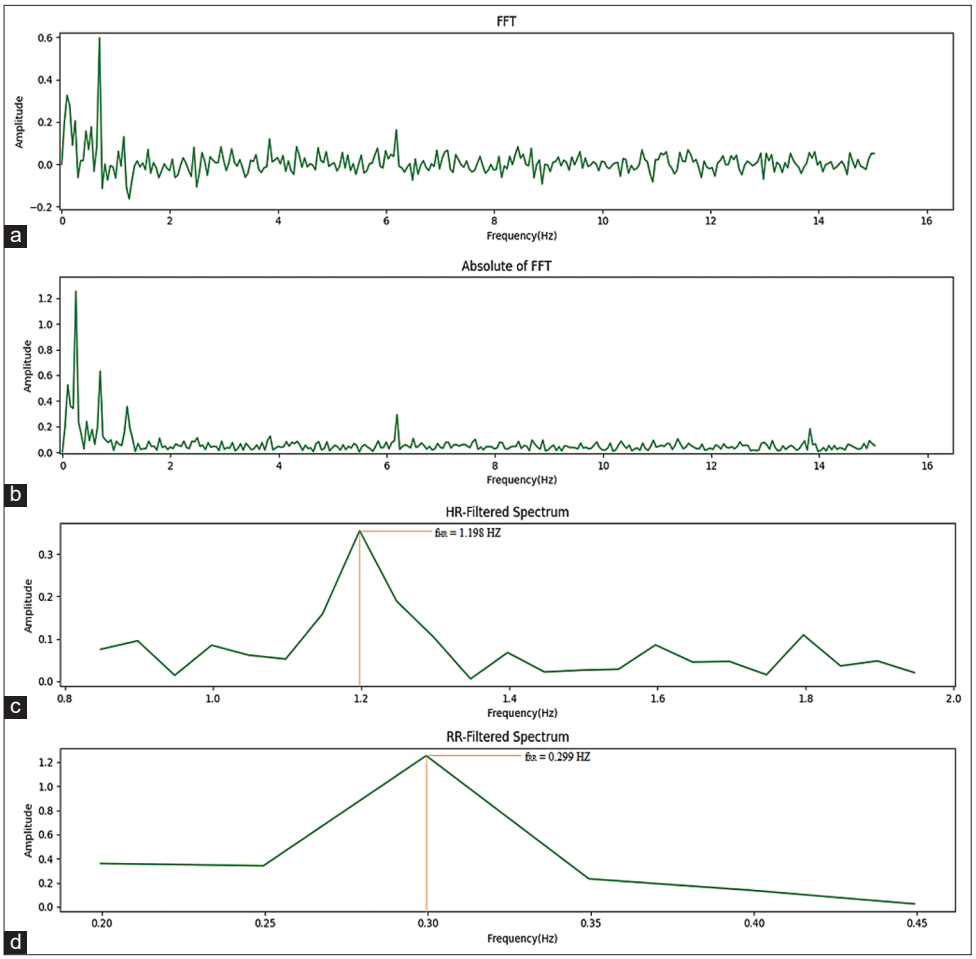

Figure 5: Frequency spectrum of the: (a) Fast Fourier transform (FFT) of the signal. (b) Absolute of FFT of the signal. (c) Heart rate-filtered signal. (d) Respiratory rate-filtered signal

$$PP\ (mmHg)=SBP-DP \quad (6)$$

PP is directly related with SV as:[82]

$$\frac{SV}{PP}=(0.013\times Weight(Kg)-0.007\times Age(y)-0.004\times HR \quad (7)$$

[25]

So, PP can be calculated from equation (7) as:

$$PP\left(mmHg\right)=\frac{SV}{\left(\begin{matrix}0.013\times\ Weight\left(Kg\right)-0.007\\ \times\ Age\left(y\right)-0.004\times\ HR\end{matrix}\right)+1.307} \quad (8)$$

Mean arterial pressure (MAP) is the average BP during one cardiac cycle. MAP is related to CO and R by a similar relationship to Ohm's law for electric current and sometimes called Darcy's la.[83] Therefore, MAP can be found by the following equation:

$$MAP\ (mmHg)=CO\times R \quad (9)$$

After finding PP and MAP values, DP founded as:[84]

$$DP(mmHg)=MAP-\frac{PP}{3} \quad (10)$$

Finally, the value of SBP is found by substituting equation (6) into equation (10):

$$SBP\ (mmHg)=3MAP-2DP \quad (11)$$

The value of R was founded through experiments, as the value that gave the best results, which is 17.52 mmHg·min/L.

Blood SpO_2

SpO_2 monitors using the same principle used in the literature[85] with some differences in methods and different tools as shown in Table 1.

In our proposed method, the amplitude and the shape of the extracted PPG signals are important to estimate the SpO_2.

First, the red and green PPG signals were normalized then filtered to reduce the noise effect by using a low-pass filter with cut-off frequencies: 2.2 Hz and 3.2 Hz, respectively. After that, the peaks in both the red and the green PPG signals were found. The peak height (Vp^{λ}) and the rising edge slope of the peak (m^{λ}), which are cleared in Figure 6, were computed to estimate the SpO_2.

Table 1: The different parameters between our study and the study in the literature[85]

Parameter	Literatures[85]	Ours
Human part	Finger (index)	Face (cheeks)
Sensor	Rear camera of a smartphone	USB webcam
Processor	Smartphone	Laptop
Software	Android application	Python script
Illumination	Led light of the smartphone	Ambient light + built-in webcam ring light
Connection	Contact	Contactless
Real-time	No	Yes
Difficulty	Low	High

The symbol λ is an indicator of whether the green PPG or the red PPG was used, where it is equal to 600 nm or 940 nm, respectively.

SpO_2 was calculated according to equation (12),[86] where $\varepsilon_{HbO2\lambda}$, and $\varepsilon_{Hb\lambda}$ refer to the absorption coefficients of HbO_2 and Hb, respectively, at wavelength λ.

$$SpO_2 = \frac{\varepsilon_{Hb_{600}}\sqrt{m_{940}\ln(Vp_{940})} - \varepsilon_{Hb_{940}}\sqrt{m_{600}\ln(Vp_{600})}}{\sqrt{m_{940}\ln(Vp_{940})}\left(\varepsilon_{Hb_{600}} - \varepsilon_{HbO2_{600}}\right) - \sqrt{m_{600}\ln(Vp_{600})}\left(\varepsilon_{Hb_{940}} - \varepsilon_{HbO2_{940}}\right)} \quad (12)$$

We optimized the SpO_2 by applying equation (14).[85] The non-normalized red, green, and blue PPG signals were used for optimization. The P^{β} terms is founded using equation (13), where β indicates the non-normalized red (R), green (G), and blue (B) PPG signals. The constant 16.53 is the mean of errors between the reference values and the results of the training signals.

$$P^{\beta} = \text{Maximum } (\beta) - \text{minimum } (\beta) \quad (13)$$

$$SpO_2\% = (SpO_2 \times 100 + (P_R \times 0.25) - (P_G \times 0.05) - (P_B \times 0.55)) - 16.53 \quad (14)$$

These methods for HR, RR, BP, and SpO_2 monitoring were applied on both recorded videos and real-time videos. In real-time monitoring, the number of fps is decreasing over time as shown in Figure 7, which is limited by: Camera frame rate, processor's number of cores, and the calculation time. The camera frame rate and the number of processor cores are constant and we cannot increase them, but we can reduce the calculation time to keep the number of fps from constantly decreasing by applying the simplest and least time-consuming monitoring methods, which is exactly what we did.

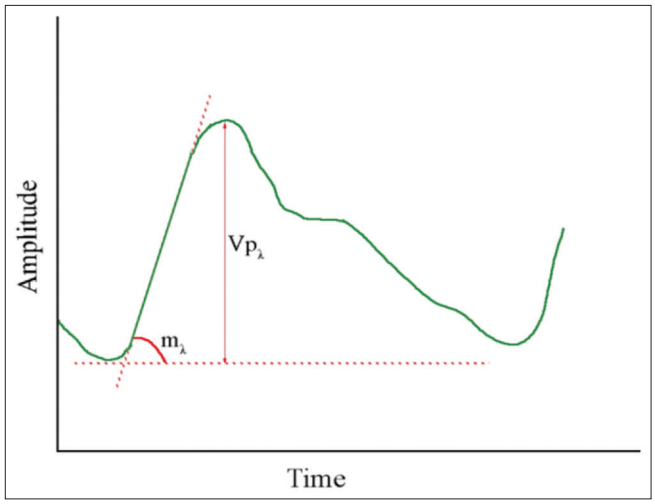

Figure 6: The slope of the rising edge (mλ) and the height of the peak (Vpλ) of a photoplethysmography signal

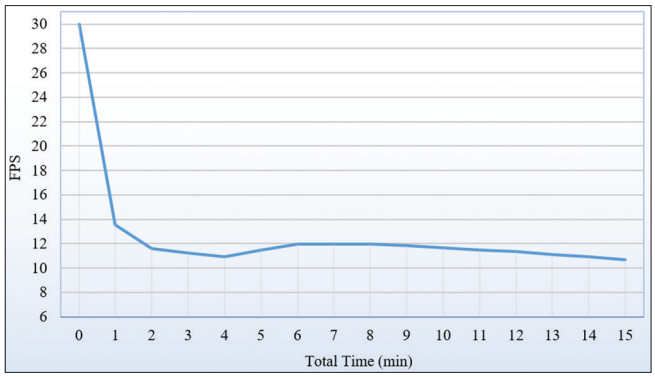

Figure 7: Number of fps during 15-min real-time monitoring

All the proposed methods were performed using python 3.8.5 with OpenCV, Numpy, Scipy, Matplotlib, and other libraries.

THE RESULTS

After applying our proposed methods to monitor HR, RR, BP, and SpO_2 on our local dataset, and comparing the results with the ground-truth, the results showed convergence with little difference between the three experiments due to the difference in illumination as shown in Tables 2-4. The maximum error was: HR ±3, RR ±2.3, SBP ±3, DP ±2, SpO_2±3.

After the success of our methods on monitoring the four vital signs on recorded videos, we apply them on real-time videos for continuous 15 min indoors with fluorescent ambient light and the second brightness of the webcam. The maximum error was: HR ±4, RR ±2.2, SBP ±3, DP ±1, SpO_2 ±2.

Table 2: The maximum error of HR, SBP, DP, and SpO_2 compared to the ground-truth, with fluorescent ambient light and the second brightness of the webcam illumination

Subject	Age	Gender	Maximum error			
			HR	SBP	DP	SpO_2
1	13	Female	2.9	2	−1	2
2	19	Male	−3	−2	−1	3
3	20	Female	−3	2	1	2
4	22	Female	1.2	−1	1	2
5	23	Female	1.4	−2	−1	1
6	25	Male	2	1	1	2
7	26	Female	2.6	2	1	−2
8	27	Female	−1.3	−1	0	1
9	52	Female	1.7	1	−1	3
10	60	Male	−2.8	−2	1	2

HR: Heart rate, RR: Respiratory rate, SpO_2: Oxygen saturation, SBP: Systolic blood pressure, DBP: Diastolic blood pressure, BP: Blood pressure

Table 3: The maximum error of HR, SBP, DP, and SpO_2 compared to the ground-truth, with indoors natural ambient light and the second brightness of the webcam illumination

Subject	Age	Gender	Maximum Error			
			HR	SBP	DP	SpO_2
1	13	Female	2.5	1	−1	1.5
2	19	Male	−2.5	−2	−1	2.2
3	20	Female	2.1	1	1	1
4	22	Female	1	−1	1	1.3
5	23	Female	2.1	−1	0	−1
6	25	Male	1.5	1	−1	−2.1
7	26	Female	−2.2	2	1	1.9
8	27	Female	−1	−1	1	1
9	52	Female	−2.5	1	−1	2.2
10	60	Male	−2.8	−2	1	2

HR: Heart rate, RR: Respiratory rate, SpO_2: Oxygen saturation, SBP: Systolic blood pressure, DBP: Diastolic blood pressure, BP: Blood pressure

Table 4: The maximum error of HR, SBP, DP, and SpO_2 compared to the ground-truth, with outdoors indirect ambient sunlight illumination

Subject	Age	Gender	Maximum error			
			HR	SBP	DP	SpO_2
1	13	Female	2	2	−1	2
2	19	Male	2.3	−2	−1	2
3	20	Female	1.9	1	0	−2.3
4	22	Female	1	−1	1	−2
5	23	Female	−2	−1	−1	−1
6	25	Male	−1	1	0	−2
7	26	Female	−2	2	1	2
8	27	Female	−1.5	−1	1	1.6
9	52	Female	−2	2	0	2.5
10	60	Male	2	−2	1	2

HR: Heart rate, RR: Respiratory rate, SpO_2: Oxygen saturation, SBP: Systolic blood pressure, DBP: Diastolic blood pressure, BP: Blood pressure

CONCLUSION

Monitoring vital signs such as HR, RR, BP, and SpO_2 are very important to ensure the safety of the individual because it is an indicator of many serious diseases whose risk can be reduced if detected early. The importance of monitoring vital signs without contact has increased in recent years with the outbreak of epidemic diseases such as the Coronavirus.

This research is concerned with monitoring these vital signs in real-time without contact and continuously by facial video, as our proposed methods have achieved good results in the monitoring. The proposed monitoring system consists of a USB webcam with attached lighting for the purpose of capturing videos and a laptop for the purpose of processing and displaying the results.

We were able to monitor the vital signs indoors and outdoors under different types of illumination, provided that they are fixed. SpO_2 measurement showed a higher sensitivity toward lighting than the rest of the vital signs, because SpO_2 monitoring is affected by the intensity of the illumination, and thus the contactless monitoring of SpO_2 is more difficult than contact monitoring, from a video.

In real-time monitoring, we encountered the issue of frames per second decreasing causing data missing and errors in results. We overcame this problem by using the simplest possible algorithms and methods to reduce the processing time, taking into account that the results were not affected by that.

Our proposed methods can be used for personal monitoring of vital signs for individuals and can also be used to ensure the safety of employees in companies and public departments.

REFERENCES

1. Paradiso R. Wearable Health Care System for Vital Signs Monitoring. Proceeding IEEE/EMBS Reg 8 International Conferenc Information Technology Applications in Biomedical ITAB, 2003-Janua(May 2003); 2003. p. 283-6.
2. Yu SN, Cheng JC. A wireless physiological signal monitoring system with integrated bluetooth and WiFi technologies. Annual International Conference of the IEEE Engineering in Medicine and Biology Society, 7 VOLS(May); 2005. p. 2203-6.
3. Scebba G, Da Poian G, Karlen W. Multispectral Video Fusion for Non-contact Monitoring of Respiratory Rate

and Apnea. IEEE Trans Biomed Eng 2021;68:350-9.
4. Da Costa G. Optical remote sensing of heartbeats. Opt Commun 1995;117:395-8.
5. Puri C, Olson L, Pavlidis I, Levine J, Starren J. StressCam: non-contact measurement of users' emotional states through thermal imaging. In: CHI'05 Extended Abstracts on Human Factors in Computing Systems; 2005. p. 1725-8.
6. Takano C, Ohta Y. Heart rate measurement based on a time-lapse image. Med Eng Phys 2007;29:853-7.
7. Duy VH, Dao TT, Kim SB, Tien NT, Zelinka I. Detecting Pulse from Head Motions Using Smartphone Camera. Vol. 415. Lecture Notes in Electrical Engineering; 2017.
8. Peng RC, Zhou XL, Lin WH, Zhang YT. Extraction of heart rate variability from smartphone photoplethysmograms. Comput Math Methods Med 2015;2015:516826.
9. Shao D, Liu C, Tsow F, Yang Y, Du Z, Iriya R, *et al*. Noncontact monitoring of blood oxygen saturation using camera and dual-wavelength imaging system. IEEE Trans Biomed Eng 2015;63:1091-8.
10. Jimenez LF, Parnandi A, Gutierrez-Osuna R. Extracting Heart Rate and Respiration Rate Using Cell Phone Camera; 2013.
11. Zhang Q, Wu Q, Zhou Y, Wu X, Ou Y, Zhou H. Webcam-based, non-contact, real-time measurement for the physiological parameters of drivers. Meas J Int Meas Confed 2017;100:311-21.
12. Guo Z, Wang ZJ, Shen Z. Physiological Parameter Monitoring of Drivers Based on Video Data and Independent Vector Analysis. In: 2014 IEEE International Conference on Acoustics, Speech and Signal Processing (ICASSP) IEEE; 2014. p. 4374-8.
13. Bousefsaf F, Maaoui C, Pruski A. Remote assessment of physiological parameters by non-contact technologies to quantify and detect mental stress states. Proceeding 2014 International Conference on Control, Decision and Information Technologies CoDIT 2014; (November); 2014. p. 719-23.
14. Scully CG, Lee J, Meyer J, Gorbach AM, Granquist-Fraser D, Mendelson Y, *et al*. Physiological parameter monitoring from optical recordings with a mobile phone. IEEE Trans Biomed Eng 2011;59:303-6.
15. Rahman H, Ahmed MU, Begum S. Non-contact physiological parameters extraction using camera. In: International Internet of Things Summit. Berlin: Springer; 2015. p. 448-53.
16. Shao D, Yang Y, Liu C, Tsow F, Yu H, Tao N. Noncontact monitoring breathing pattern, exhalation flow rate and pulse transit time. IEEE Trans Biomed Eng 2014;61:2760-7.
17. Ali DH, Aziz MH. A Survey on Non-Contact Heart Rate Estimation from Facial Video; 2021. p. 1-15.
18. RxList. Medical Definition of Heart Rate. Available from: https://www.rxlist.com/heart_rate/definition.htm [Last accessed on 2021 Aug 26].
19. The Free Dictionary. Doppler Probe. Available from: https://medical-dictionary.thefreedictionary.com/Doppler+probe [Last accessed on 2021 Aug 25].
20. Nonin. What Is a Pulse Oximeter. Available from: https://www.nonin.com/resource/what-is-a-pulse-oximeter [Last accessed on 2021 Aug 25].
21. NHS. Electrocardiogram (ECG). Available from: https://www.nhs.uk/conditions/electrocardiogram [Last accessed on 2021 Aug 25].
22. Scanlon VC, Sanders T. Essentials of Anatomy and Physiology. Philadelphia, PA: FA Davis; 2018.
23. Fleming S, Thompson M, Heneghan C, Maconochie I. Normal ranges of heart rate and respiratory rate in children from birth to 18 years: A systematic review of observational studies. Lancet 2011;377:1011-8.
24. Poh MZ, McDuff DJ, Picard RW. Advancements in noncontact, multiparameter physiological measurements using a webcam. IEEE Trans Biomed Eng 2010;58:7-11.
25. Li X, Chen J, Zhao G, Pietikäinen M. Remote Heart Rate Measurement from Face Videos under Realistic Situations. Proceeding IEEE Computer Society Conference on Computer Vision and Pattern Recognition November; 2018. p. 4264-71.
26. Carvalho L, Virani M, Kutty M. Analysis of heart rate monitoring using a webcam. Analysis 2014;3:6593-5.
27. Rahman H, Ahmed MU, Begum S, Funk P. Real Time Heart Rate Monitoring from Facial RGB Color Video Using Webcam. In: The 29th Annual Workshop of the Swedish Artificial Intelligence Society (SAIS), 2-3 June 2016, Malmö, Sweden Linköping University Electronic Press; 2016.
28. Bai G, Huang J, Liu H. Real-time robust noncontact heart rate monitoring with a camera. IEEE Access 2018;6:33682-91.
29. Ghanadian H, Al Osman H. Non-contact Heart Rate Monitoring Using Multiple RGB Cameras. Lecture Notes in Computer Science (Including Subseries Lecture Notes in Artificial Intelligence and Lecture Notes Bioinformatics) 2019, No. 11679 LNCS October; 2019. p. 85-95.
30. Zhao C, Lin CL, Chen W, Chen MK, Wang J. Visual heart rate estimation and negative feedback control for fitness exercise. Biomed Signal Process Control 2020;56:101680.
31. Negishi T, Abe S, Matsui T, Liu H, Kurosawa M, Kirimoto T, *et al*. Contactless vital signs measurement system using RGB-thermal image sensors and its clinical screening test on patients with seasonal influenza. Sensors 2020;20:2171.
32. De Haan G, Jeanne V. Robust pulse rate from chrominance-based rPPG. IEEE Trans Biomed Eng 2013;60:2878-86.
33. Sun G, Nakayama Y, Dagdanpurev S, Abe S, Nishimura H, Kirimoto T, *et al*. Remote sensing of multiple vital signs using a CMOS camera-equipped infrared thermography system and its clinical application in rapidly screening patients with suspected infectious diseases. Int J Infect Dis 2017;55:113-7.
34. Sanyal S, Nundy KK. Algorithms for monitoring heart rate and respiratory rate from the video of a user's face. IEEE J Transl Eng Heal Med 2018;6:2818687.
35. MedicineNet. Medical Definition of Respiratory Rate. Available from: https://www.medicinenet.com/respiratory_rate/definition.htm [Last accessed on

2021 Aug 26].
36. Cleveland Clinic. Vital Signs. Available from: https://my.clevelandclinic.org/health/articles/10881-vital-signs [Last accessed on 2021 Aug 26].
37. Yuan G, Drost N, McIvor R. Respiratory rate and breathing pattern. MumjOrg 2013;10(1):23-5.
38. Singh G, Tee A, Trakoolwilaiwan T, Taha A, Olivo M. Method of respiratory rate measurement using a unique wearable platform and an adaptive optical-based approach. Intensive Care Med Exp 2020;8:1-9.
39. Wu D, Yang P, Liu GZ, Zhang YT. Automatic estimation of respiratory rate from pulse transit time in normal subjects at rest. Proceeding IEEE-EMBS International Conference on Biomedical and Health Informatics Global Gd Chall Health Informatics, BHI; 2012. p. 779-81.
40. Yilmaz T, Foster R, Hao Y. Detecting vital signs with wearablewireless sensors. Sensors 2010;10:10837-62.
41. Simoes EA, Roark R, Berman S, Esler LL, Murphy J. Respiratory rate: Measurement of variability over time and accuracy at different counting periods. Arch Dis Child 1991;66:1199-203.
42. Ge L, Zhang J, Wei J. Single-frequency ultrasound-based respiration rate estimation with smartphones. Comput Math Methods Med 2018;2018:3675974.
43. Arlotto P, Grimaldi M, Naeck R, Ginoux JM. An ultrasonic contactless sensor for breathing monitoring. Sensors (Switzerland) 2014;14:15371-86.
44. Dang TT, Tran KQN, Le HM, Tran K, Dinh A. A Tool Using Ultrasonic Sensor for Measuring Breathing Rate. In: International Conference on the Development of Biomedical Engineering in Vietnam Cham: Springer International Publishing; 2018. p. 139-43.
45. Al-Naji A, Al-Askery AJ, Gharghan SK, Chahl J. A system for monitoring breathing activity using an ultrasonic radar detection with low power consumption. J Sens Actuator Netw 2019;8:1-17.
46. Shahshahani A, Bhadra S, Zilic Z. A continuous respiratory monitoring system using ultrasound piezo transducer. Proceeding IEEE International Symposium on Circuits and Systems; 2018. p. 18-21.
47. Wang T, Zhang D, Wang L, Zheng Y, Gu T, Dorizzi B, *et al*. Contactless respiration monitoring using ultrasound signal with off-the-shelf audio devices. IEEE Internet Things J 2019;6:2959-73.
48. Dei D, Grazzini G, Luzi G, Pieraccini M, Atzeni C, Boncinelli S, *et al*. Non-contact detection of breathing using a microwave sensor. Sensors (Switzerland) 2009;9:2574-85.
49. Becker C, Achermann S, Rocque M, Kirenko I, Schlack A, Dreher-Hummel T, *et al*. Camera-based measurement of respiratory rates is reliable. Eur J Emerg Med 2018;25:416-22.
50. Benetazzo F, Freddi A, Monteriù A, Longhi S. Respiratory rate detection algorithm based on RGB-D camera: Theoretical background and experimental results. Healthc Technol Lett 2014;1:81-6.
51. Chan P, Wong G, Nguyen TD, Nguyen T, McNeil J, Hopper I. Estimation of respiratory rate using infrared video in an inpatient population: an observational study. J Clin Monit Comput 2020;34:1275-84.
52. Procházka A, Charvátová H, Vyšata O, Kopal J, Chambers J. Breathing analysis using thermal and depth imaging camera video records. Sensors (Switzerland) 2017;17:1-10.
53. Massaroni C, Lopes DS, Lo Presti D, Schena E, Silvestri S. Contactless monitoring of breathing patterns and respiratory rate at the pit of the neck: A single camera approach. J Sensors 2018;2018:4567213.
54. Makkapati VV, Rambhatla SS. Remote Monitoring of Camera Based Respiration Rate Estimated by Using Occlusion of Dot Pattern. 2016 IEEE International Conference on Advanced Networks and Telecommunications Systems ANTS 2016; 2017.
55. Elphick HE, Alkali AH, Kingshott RK, Burke D, Saatchi R. Exploratory study to evaluate respiratory rate using a thermal imaging camera. Respiration 2019;97:205-12.
56. Pereira CB, Yu X, Czaplik M, Rossaint R, Blazek V, Leonhardt S. Remote monitoring of breathing dynamics using infrared thermography. Biomed Opt Express 2015;6:4378.
57. Al-Kalidi F, Elphick H, Saatchi R, Burke D. Respiratory rate measurement in children using a thermal camera. Int J Sci Eng Res 2015;6:1748-56.
58. Cho Y, Julier SJ, Marquardt N, Bianchi-Berthouze N. Robust tracking of respiratory rate in high-dynamic range scenes using mobile thermal imaging. Biomed Opt Express 2017;8:4480.
59. Hwang H, Lee EC. Non-contact respiration measurement method based on rgb camera using 1d convolutional neural networks. Sensors 2021;21:3456.
60. Jakkaew P, Onoye T. Non-contact respiration monitoring and body movements detection for sleep using thermal imaging. Sensors (Switzerland) 2020;20:1-14.
61. NHS. What is Blood Pressure? Available from: https://www.nhs.uk/common-health-questions/lifestyle/what-is-blood-pressure [Last accessed on 2021 Aug 26].
62. Conduct Science. A Comprehensive Guide to Sphygmomanometers. Available from: https://conductscience.com/a-comprehensive-guide-to-sphygmomanometers [Last accessed on 2021 Aug 26].
63. Sugita N, Yoshizawa M, Abe M, Tanaka A, Homma N, Yambe T. Contactless technique for measuring blood-pressure variability from one region in video plethysmography. J Med Biol Eng 2019;39:76-85.
64. Jain M, Deb S, Subramanyam A V. Face Video Based Touchless Blood Pressure and Heart Rate Estimation. 2016 IEEE 18th International Work Multimed Signal Process MMSP 2016; 2017.
65. Secerbegovic A, Bergsland J, Halvorsen PS, Suljanovic N, Mujcic A, Balasingham I. Blood Pressure Estimation Using Video Plethysmography. IEEE 13th International Symposium on Biomedical Imaging; 2016. p. 461-4.
66. Huang PW, Lin CH, Chung ML, Lin TM, Wu BF. Image Based Contactless Blood Pressure Assessment Using Pulse Transit Time; 2017 International Automatic Control Conference CACS; 2018. p. 1-6.
67. Jeong IC, Finkelstein J. Introducing contactless blood pressure assessment using a high speed video camera. J Med Syst 2016;40:1-10.
68. Sugita N, Obara K, Yoshizawa M, Abe M, Tanaka A, Homma N. Techniques for Estimating Blood Pressure

Variation Using Video Images. proceedings under Annual International Conference of the IEEE Engineering in Medicine and Biology Society EMBS; 2015. p. 4218-21.
69. Wang LV, Gao L. Photoacoustic microscopy and computed tomography: From bench to bedside. Ann Rev Biomed Eng 2014;16:155-8.
70. Reddy KA, George B, Mohan NM, Kumar VJ. A novel calibration-free method of measurement of oxygen saturation in arterial blood. IEEE Trans Instrum Meas 2009;58:1699-705.
71. Chan ED, Chan MM, Chan MM. Pulse oximetry: Understanding its basic principles facilitates appreciation of its limitations. Respir Med 2013;107:789-99.
72. Nitzan M, Romem A, Koppel R. Pulse oximetry: Fundamentals and technology update. Med Devices Evid Res 2014;7:231-9.
73. iWorx. Pulse Oximeters and Sensors. iWorx Syst Inc.; 2012.
74. Radiometer MA. ABL800 Flex Manual; 2012.
75. Scharf JE. Green light pulse oximeter. Tampa, FL, United States: University of South Florida; 1998.
76. Prahl S. Optical Absorption of Hemoglobin. Available from: https://omlc.org/spectra/hemoglobin [Last accessed on 2021 Aug 24].
77. Verkruysse W, Svaasand LO, Nelson JS. Remote plethysmographic imaging using ambient light. Opt Express 2008;16:21434-45.
78. Webster JG. Design of Pulse Oximeters. Boca Raton: CRC Press; 1997.
79. Asthana A, Zafeiriou S, Cheng S, Pantic M. Robust Discriminative Response Map Fitting with Constrained Local Models. Proceedings of the IEEE Computer Society Conference on Computer Vision and Pattern Recognition; 2013. p. 3444-51.
80. Tarassenko L, Villarroel M, Guazzi A, Jorge J, Clifton DA, Pugh C. Non-contact video-based vital sign monitoring using ambient light and auto-regressive models. Physiol Meas 2014;35:807-31.
81. Fay DL. Anesthesia secrets. Angew Chem Int Ed 2020;6:951-2.
82. De Simone G, Roman MJ, Koren MJ, Mensah GA, Ganau A, Devereux RB. Stroke volume/pulse pressure ratio and cardiovascular risk in arterial hypertension. Hypertension 1999;33:800-5.
83. Mayet J, Hughes A. Cardiac and vascular pathophysiology in hypertension. Heart 2003;89:1104-9.
84. Value N, Used P. Review of Medical Physiology. 23rd ed. New York: McGraw-Hill; 2009.
85. Nemcova A, Jordanova I, Varecka M, Smisek R, Marsanova L, Smital L, *et al*. Monitoring of heart rate, blood oxygen saturation, and blood pressure using a smartphone. Biomed Signal Process Control 2020;59:101928.
86. Lamonaca F, Carni DL, Grimaldi D, Nastro A, Riccio M, Spagnolo V. Blood Oxygen Saturation Measurement by Smartphone Camera. 2015 International Symposium on Medical Measurements Applications MeMeA; 2015. p. 359-64.